PROCEEDINGS OF THE ROYAL SOCIETY B BIOLOGICAL SCIENCES

# Morphological innovation, diversification and invasion of a new adaptive zone

Elizabeth R. Dumont, Liliana M. Dávalos, Aaron Goldberg, Sharlene E. Santana, Katja Rex and Christian C. Voigt

*Proc. R. Soc. B* 2012 **279**, 1797-1805 first published online 23 November 2011
doi: 10.1098/rspb.2011.2005

PROCEEDINGS OF THE ROYAL SOCIETY B

*Proc. R. Soc. B* (2012) **279**, 1797–1805
doi:10.1098/rspb.2011.2005
*Published online* 23 November 2011

# Morphological innovation, diversification and invasion of a new adaptive zone

**Elizabeth R. Dumont[1,2,*,†], Liliana M. Dávalos[3,4,*,†], Aaron Goldberg[3], Sharlene E. Santana[2,5], Katja Rex[6] and Christian C. Voigt[6]**

[1]*Department of Biology, and* [2]*Graduate Program in Organismic and Evolutionary Biology, 221 Morrill Science Center, University of Massachusetts, Amherst, MA 01003, USA*
[3]*Department of Ecology and Evolution, Stony Brook University, 650 Life Sciences Building, Stony Brook, NY 11794, USA*
[4]*Consortium for Inter-Disciplinary Environmental Research, School of Marine and Atmospheric Sciences, Stony Brook University, 129 Dana Hall, Stony Brook, NY 11794, USA*
[5]*Center for Society and Genetics, University of California Los Angeles, Box 957221, 1323 Rolfe Hall, Los Angeles, CA 90095, USA*
[6]*Leibniz Institute for Zoo and Wildlife Research, Research Group in Evolutionary Ecology, Alfred-Kowalke-Str. 17, 10315 Berlin, Germany*

How ecological opportunity relates to diversification is a central question in evolutionary biology. However, there are few empirical examples of how ecological opportunity and morphological innovation open new adaptive zones, and promote diversification. We analyse data on diet, skull morphology and bite performance, and relate these traits to diversification rates throughout the evolutionary history of an ecologically diverse family of mammals (Chiroptera: Phyllostomidae). We found a significant increase in diversification rate driven by increased speciation at the most recent common ancestor of the predominantly frugivorous subfamily Stenodermatinae. The evolution of diet was associated with skull morphology, and morphology was tightly coupled with biting performance, linking phenotype to new niches through performance. Following the increase in speciation rate, the rate of morphological evolution slowed, while the rate of evolution in diet increased. This pattern suggests that morphology stabilized, and niches within the new adaptive zone of frugivory were filled rapidly, after the evolution of a new cranial phenotype that resulted in a certain level of mechanical efficiency. The tree-wide speciation rate increased non linearly with a more frugivorous diet, and was highest at measures of skull morphology associated with morphological extremes, including the most derived Stenodermatines. These results show that a novel stenodermatine skull phenotype played a central role in the evolution of frugivory and increasing speciation within phyllostomids.

**Keywords:** diversification; morphological innovation; bats; frugivory

## 1. INTRODUCTION

Why do some lineages comprise many species and a wide range of ecological variation, while others encompass only few species that vary little from one another [1]? Ecological opportunity unlocked by morphological innovations, the invasion of a new environment, or the extinction of competitors and predators can unleash higher rates of speciation and/or lower extinction rates and explain observed disparities in taxonomic and ecological diversity [2–4]. Documenting shifts in diversification rates is now possible across large swaths of the Tree of Life thanks to new phylogenetic approaches coupled with robust estimates of divergence times (e.g. mammals and warblers [5,6]). It has been more difficult to test the role of ecological opportunity and its mechanism in shifts in diversification rates [7,8]. Morphological innovations have been discussed extensively as drivers of diversification (e.g. [7,9–11]), but close inspection tends to reveal either small effects or alternative mechanisms of exploiting ecological opportunity (e.g. neither pharyngeal jaws in labrid fishes nor nectar spurs in *Halenia* are associated with higher diversification rates [12,13]). It has proved hard to show that traits proposed as morphological innovations confer advantage in exploiting ecological opportunity, and this is critical to demonstrating diversification through morphological innovation [14,15].

Connecting ecological opportunity to morphological change and diversification requires demonstrating that: (i) there was a significant increase in diversification rate in the lineage of interest [9]; (ii) increased diversification rate is associated with movement into a new adaptive zone; (iii) there was a change in phenotype [10]; (iv) the new phenotype improves performance in the new adaptive zone [7]; and (v) the evolution of the novel morphology and shift to the new adaptive zone are associated with increases in diversification rate [16]. To date, few analyses have

*Authors for correspondence (bdumont@bio.umass.edu; ldavalos@life.bio.sunysb.edu).
†These authors contributed equally to this work.

Electronic supplementary material is available at http://dx.doi.org/10.1098/rspb.2011.2005 or via http://rspb.royalsocietypublishing.org.

*Received* 24 September 2011
*Accepted* 3 November 2011

examined the connection between ecological opportunity and diversification [12], and even fewer have linked phenotype to performance in this context [17,18].

Here, we analyse large and comprehensive datasets summarizing diet, cranial morphology, and bite force from one of the most ecologically diverse families of mammals (Chiroptera: Phyllostomidae, 180 species) to elucidate drivers and mechanisms of diversification. In particular, we test the hypothesis that the evolution of frugivory and a skull phenotype that improved biting performance within this feeding habit is associated with increasing diversification rates in this family. Outgroups to phyllostomids and basal members of the family are insectivorous. Although a few phyllostomid species are omnivorous and/or eat soft fruits, only members of the subfamily Stenodermatinae are primarily frugivorous and regularly consume relatively hard canopy fruits, especially figs [19,20]. The evolution of frugivory is thought to have promoted diversification in phyllostomids by opening a new adaptive zone [21]. Studies of whole-organism performance in bats have uncovered strong correlations between diet (ecology), skull morphology (phenotype) and bite force (feeding performance) [22–24], suggesting a possible mechanism of adaptive ecological diversification through morphological innovation. Despite patterns of species diversity consistent with ecological drivers [25], the roles of ecological opportunity, phenotypic innovation and performance in taxonomic diversification have not been established because quantitative data have been lacking.

We evaluated five predictions that arise from the hypothesis that feeding on relatively hard canopy fruits represented a new adaptive zone accessed through the evolution of skull morphology, and led to a significant increase in diversification rate (i.e. the rate of increase in accumulation of new lineages brought about by an increase in speciation, a decrease in extinction, or a combination of both). First, there should be evidence of a significant shift in diversification rate at the base of the frugivorous clade [26,27]. Second, diet and skull morphology should be significantly linked. Third, there should be a significant association between skull morphology and enhanced biting performance in the new adaptive zone [23,28]. Fourth, if morphological innovation opened the door to the new adaptive zone and increased diversification, the rate of trophic evolution should increase as the new adaptive zone is filled, while the rate of morphological evolution should decrease as the innovation is maintained within the clade by stabilizing selection [29]. Fifth, tree-wide diversification rates should be significantly linked to diet and skull morphology. These analyses link higher speciation rates to the evolution of both frugivory and a skull phenotype that improved biting performance when eating fruit, demonstrating the role of ecological opportunity and morphological innovation in promoting diversification.

## 2. METHODS

### (a) *Phylogeny estimation and evolutionary timeline*

We estimated phylogenies by analysing partial sequences of four mitochondrial genes: 12S and 16S ribosomal RNA, cytochrome *b*, cytochrome oxidase I; and the autosomal recombination activating gene 2 from 150 ingroup species exemplars [30]. Homologous sequences of closely related families (*Mormoops*, *Pteronotus*, *Noctilio* and *Mystacina)* were used to root the tree [31]. Sequences were collected from GenBank and aligned using the perl script TransAlign v. 1.2 [32] for protein-coding genes, and Mafft v. 6.611b with the Q-INS-i algorithm [33] for mitochondrial ribosomal loci. The flanks of the resulting alignments were trimmed to minimize missing data, yielding a final supermatrix of 4840 nucleotides.

To identify the best partitioning scheme for phylogenetic analyses of the supermatrix, we calculated the Bayesian Information Criterion (BIC) and rescaled Akaike information criterion (AIC*c*) [34] of six alternative partition sets based on the harmonic mean of the posterior log-likelihoods (HMLL) of parallel MrBayes v. 3.2 [35] Metropolis coupled Markov chain Monte Carlo (MCMCMC) searches. These searches were conducted in three steps: (i) one maximum likelihood (ML) tree was obtained by choosing from 100 phylogenetic inferences of the non-partitioned data with independent random starting trees in RAxML v. 7.0.48 [36]; (ii) the best-fit model of sequence evolution for each partition was selected via the AIC*c* calculated in MrAIC.pl v. 1.4.4 [37,38]; and (iii) parameters of the best-fit model of sequence evolution for each partition and tree branch lengths were allowed to vary in MrBayes searches (10 million generations, four chains), with the tree constrained to the single ML topology within each partitioning scheme.

We used relaxed molecular clock and fossil calibrations to obtain time-calibrated phylogenies by: (i) running 50 independent RAxML searches with the best partition scheme to obtain a ML estimate of phylogeny; (ii) selecting the best tree model in many-core parallel Beast v. 1.6.1 [39,40] with the ML phylogeny as the starting tree; and (iii) applying the best tree model in parameter and tree searches in Beast. The best fit between the pure-speciation (Yule) and birth–death (speciation–extinction) model was evaluated in Beast by running 20 million generations in MCMCMC searches. To constrain divergence times, we used a prior on the age of the root based on published estimates [41,42] and nine fossil calibration points distributed throughout the tree (see electronic supplementary material, figure S1 and table S1), and drawing per-branch rates of molecular evolution from a lognormal distribution [43]. After selecting the best tree model, we ran four separate 20-million generation Beast searches with the same starting tree, calibration points and relaxed clock model. No topological constraints were enforced and all parameters were sampled every 1000 generations. Convergence in log-likelihoods (LLs) and parameter autocorrelation times were evaluated using Tracer v. 1.5 [44].

### (b) *Model comparisons*

Having a large sample of dated phylogenies enabled us to measure the impact of variation in branch lengths and tree topologies on all subsequent comparative analyses: diversification rate, trait evolution, regressions between traits and models of diversification as a function of trait evolution. We adopted a likelihood-based approach to scaling up hypothesis testing in series of more than or equal to 100 trees (in most cases 1000) without incurring in greater-than-nominal type-I error. In analyses applying ML optimization, this was achieved by conducting likelihood ratio tests (LRTs) between the HMLLs of nested models with degrees of freedom equal to the difference in the number of parameters between the models. In Bayesian Markov chain Monte Carlo (MCMC) analyses, the marginal log-likelihoods were

approximated by calculating the HMLLs of each series of posterior uncorrelated parameter samples, and using these in LRTs, as above. Finally, non-nested models were compared using the $AIC_{HMLL}$, and the criteria of [45]: models within two AIC units of the lowest AIC are supported by the data, while models with more than four units difference were discounted. Unless expressly noted, all analyses were performed in the R statistical language [46].

### (c) *Diversification rates*

With thousands of dated phylogenies in hand, our next goal was to determine where in each tree the greatest shift in diversification rate occurred. We used a combination of ML and MCMC approaches to test for the presence of shifts in diversification rate in each tree. To identify the node with the largest shift in speciation rate (and highest increase in model fit), we began by fitting models with 1 and 2 speciation rates to each of 1000 uncorrelated dated trees using the Laser R package [47] and accounting for missing species by attaching missing species as polytomies to their closest sampled relative (see the electronic supplementary material, table S2). We then fitted birth–death and pure-speciation models to each tree, using ML in the R package Diversitree (v. 0.7-7 [48]), accounting for missing species as in Laser analyses. After establishing which of the pure-speciation and birth–death models best fitted the phylogenies, we tested for a change in speciation rate at the node identified using Laser by fitting ML models. Finally, we applied a Bayesian approach to testing the significance of diversification rate change by sampling MCMC chains of 250 steps per tree. We used ML estimates of the parameters as starting points, and flat priors for speciation rates in Diversitree. The Coda package [49] was used to calculate autocorrelation times and effective sampling sizes of the MCMC samples of speciation rates.

### (d) *Trait evolution*

We collected data on the diet, skull morphology and biting performance of phyllostomid species. For diet, individual faecal samples were analysed using a blind protocol [50]. Samples consisting solely of fruit and fruit parts were assigned to trophic level 1, those consisting of only insect parts to trophic level 2 and those containing only vertebrate remains to trophic level 3. Intermediate values were common and were assigned according to the relative volume of fruit, insect and vertebrate material in the faecal sample. Variation in trophic level values among individuals yielded a continuous distribution of species means for trophic level that ranged between 1 and 2.18 (see the electronic supplementary material, table S3). Trophic level was treated as a continuous variable in subsequent analyses.

To quantify skull morphology, we measured 10 linear variables reflecting skull form (table 1) in 611 individuals of 85 species, 83 of which were sampled in the phylogeny (see the electronic supplementary material, table S4). After adding a constant (0.6) to make all observed values positive (values for one variable were both positive and negative), the raw data were size-adjusted by dividing each value for an individual by the geometric mean of values for that individual [51]. We applied a principal component (PC) analysis with Varimax rotation to the correlation matrix of the species means to construct statistically independent vectors (PCs) that summarize variation in skull morphology among species. These PC scores were used to represent morphology in subsequent analyses.

Studies of whole-organism performance in bats have established that bite force is a good measure of feeding performance and that high bite forces allow access to hard foods, including fruits [22,24]. We measured *in vivo* bite forces at intermediate gape angles from 563 individuals of 39 wild-caught bat species using a piezoelectric force transducer mounted between two bite plates [23,24,52]. We also measured head height of each individual to represent head size [53]. The maximum bite forces from individuals were averaged to obtain species means (see the electronic supplementary material, table S4).

Table 1. Eigenvalues, variance components, and factor loadings for a principal components (PC) analysis of species means of size-adjusted morphological variables. (The highest factor loading for each variable is in bold.)

| | PC1 | PC2 | PC3 |
|---|---|---|---|
| eigenvalues | 4.89 | 2.34 | 1.13 |
| % of variance | 49 | 24 | 11 |
| factor loadings | | | |
| zygomatic breadth | −0.174 | **0.821** | 0.427 |
| skull length | **0.906** | 0.148 | −0.261 |
| posterior skull width | 0.460 | **0.835** | −0.077 |
| temporal fossa diameter | −0.092 | −0.003 | **0.903** |
| skull height | **−0.830** | −0.371 | −0.270 |
| palate width at M1 | 0.127 | **0.885** | 0.012 |
| condyle height | **−0.778** | −0.005 | 0.441 |
| coronoid process elevation | **0.810** | 0.369 | 0.137 |
| condyle to M1 distance | **0.913** | −0.012 | −0.221 |
| square root of M1 area | −0.278 | **−0.677** | 0.348 |

If the availability of fruit provided the ecological opportunity that, in the presence of the morphological innovation allowing its exploitation, led to a significant increase in taxonomic diversification rates; then skull morphology (PC scores) should predict both trophic level and feeding performance (bite force). We tested these predictions using random samples of dated trees ($n = 1000$). We modelled both trophic level and bite force as functions of skull morphology (PC1 and PC2 scores) using generalized least squares (GLS) and phylogeny-based correlation structures for errors to account for shared evolutionary history [54]. To account for the effects of body size in the analyses of bite force, we included head size as an independent variable. We used R package APE [55] to obtain correlation structure matrices for each tree and applied them in GLS models fitted using ML in nlme [56]. The most appropriate correlation structure for the residuals of the regression on each tree was determined by comparing the fit of Brownian motion (BM) or BM plus the scaling parameter $\lambda$ [57] models using LRTs.

If changes in skull morphology opened the door to ecological opportunity and taxonomic diversification, then a shift in species diversification rate should be associated with a deceleration in the rate of morphological evolution and an acceleration in the rate of trophic evolution as the new adaptive zone is filled [29]. For a sample of 1000 dated phylogenies pruned to match either the trophic level or morphological data (PC scores), we divided each phylogeny into one paraphyletic group and one monophyletic group: the clades above and below the node at which the largest change in taxonomic diversification rate occurred. For each tree, we then used the program Brownie [58] to fit a null model of a single rate of trait change across the tree, and a censored model with a different rate in each of the two groups. Finally, we evaluated whether the two groups differed by comparing trophic level between the two groups. We used 1000 randomly selected

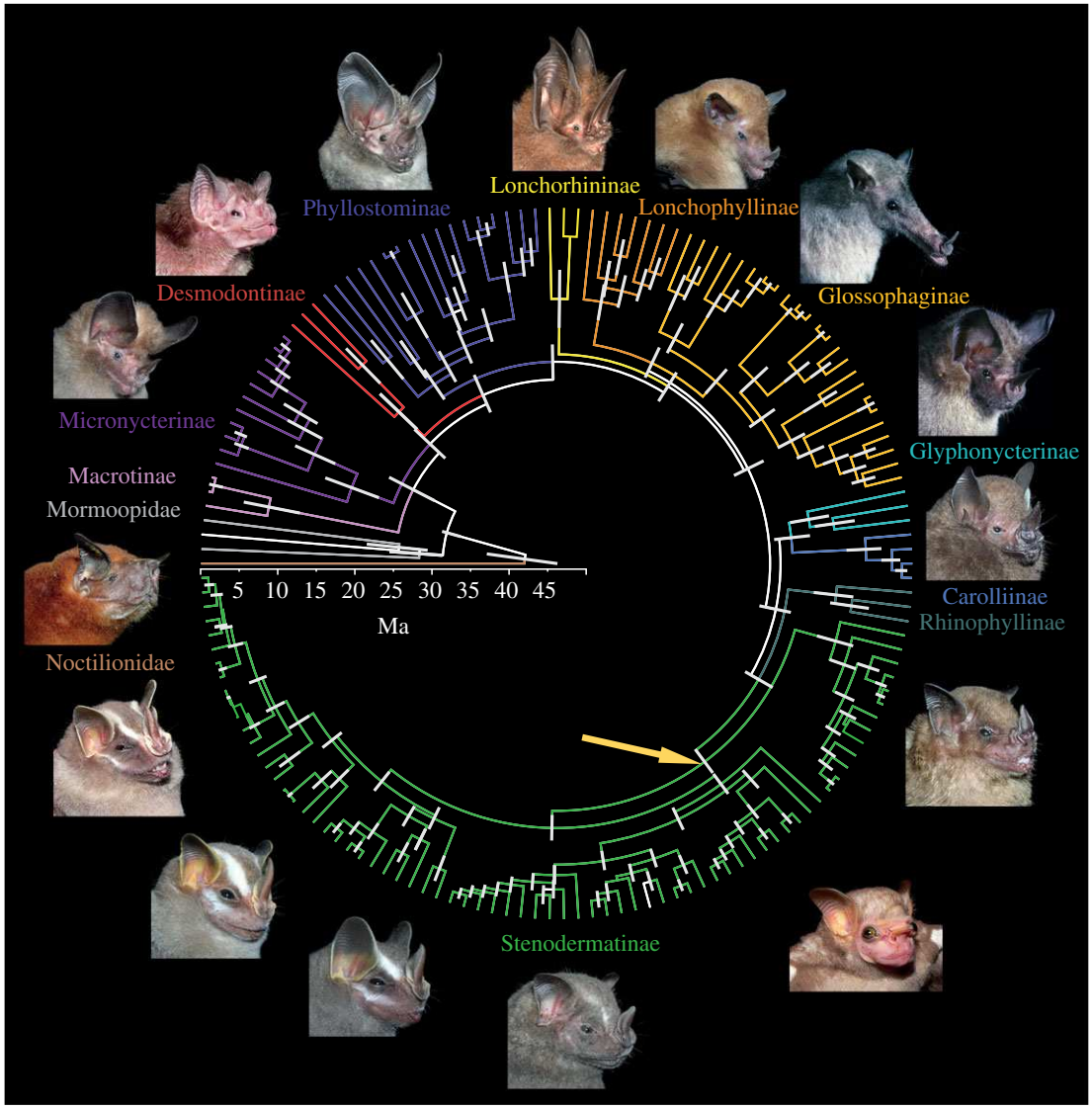


Figure 1. Summary phylogeny of 150 species of phyllostomid bats illustrating diversity in lineages and morphology among subfamilies. Branch lengths are proportional to time and grey bars indicate 95% confidence intervals (CI) around node dates. The yellow arrow indicates the node where the largest shift in species diversification rate was found. Clockwise from top species are: *Lonchorhina aurita*, *Lonchophylla robusta*, *Musonycteris harrisoni*, *Glyphonycteris silvestris*, *Carollia castanea*, *Sturnira lilium*, *Sphaeronycteris toxophyllum*, *Artibeus jamaicensis*, *Uroderma bilobatum Vampyressa pusilla*, *Platyrrhinus umbratus*, *Noctilio albiventris* (outgroup), *Micronycteris hirsuta*, *Desmodus rotundus*, *Lophostoma silvicolum*.

trees to account for correlated error structures, and tested the hypothesis of difference in mean trophic level between groups.

### (e) *Relationship between diversification and trait evolution*

We evaluated the relationships between diet (trophic level) and skull morphology (PC1 scores) and diversification rates by comparing 10 linear and nonlinear models of speciation as a function of the evolution of each trait across one randomly selected phylogeny in DIVERSITREE [48,59]. The null models had constant speciation and extinction rates (birth–death) independent of trait evolution, with increasingly complex linear and nonlinear functions of speciation rates (extinction rates remained fixed, see [48]) as a function of traits. A directional parameter of trait evolution was also included in these models.

We modelled diversification rates as a diffusion process function of each of the traits, and this required standard deviations to account for intraspecific variation. We obtained per-species standard deviations of trophic level from individual samples and used the median of the per-species standard deviation in the six species for which only one individual was available (see the electronic supplementary material, table S3). To generate standard deviations of PC scores, we bootstrapped without replacement the samples of morphological measurements, yielding 100 replicates of the morphological dataset. We then extracted PC scores from each dataset, from which we calculated the mean and standard deviation of the per-species scores. Based on the single-tree preliminary results, null models and models within two units of the lowest AIC were fitted to a random sample of 100 phylogenies using DIVERSITREE [48]. Missing species were accounted for by specifying the proportion of species not sampled in the phylogeny.

## 3. RESULTS

### (a) *Phyllostomid phylogeny and diversification rates*

Both the AIC*c* and the BIC suggested the best partitioning approach involved seven partitions, each with its own model (see the electronic supplementary material,

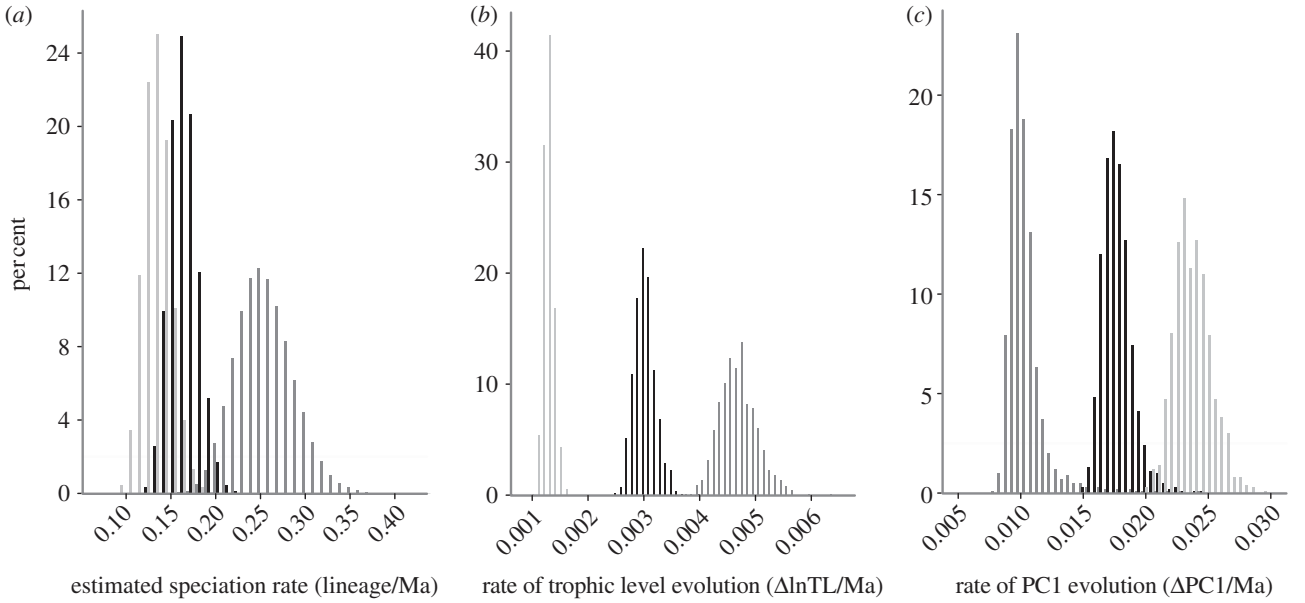


Figure 2. Frequency distributions derived from analyses of 1000 phylogenies. (*a*) MCMC sampling of birth rates across whole phylogenies, (*b*) rates of evolution of PC1 and (*c*) ln trophic level for the Phyllostomidae (black bars) as a whole, the subfamily Sternodermatinae (dark grey bars) and non-stenodermatine (light grey bars) phyllostomids.

table S5). A pure-speciation branching process could not be rejected ($\chi^2_1 = 0.63$, $p = 0.366$), so BEAST analyses were run with a pure-speciation model. Four separate BEAST runs converged after 10 million generations, with autocorrelation times of approximately 12 000. The 50 per cent posterior probability summary of 3625 uncorrelated, posterior dated trees is summarized in figure 1 (for Bayesian posterior probabilities of branches, see the electronic supplementary material, figure S2). Analyses of a random sample of 1000 uncorrelated trees using LASER overwhelmingly localized the greatest shift in speciation rates (97.3% of trees) at the base of the phyllostomid subfamily Stenodermatinae (figure 1). Birth–death models did not significantly improve the fit of diversification models to the trees ($\chi^2_1 = 0.0014$, $p \geq 0.9701$). After discarding burn-in and thinning the sample to minimize autocorrelation in pure-speciation estimates, the posterior samples comprised 123 000 estimates (down from 250 steps × 1000 trees = 250 000 estimates) of posteriors of 1- and 2-speciation rates. The 2-speciation rate model was significantly better than the single-rate model ($\chi^2_1 = 15.01$, $p = 5.66\text{E-}5$), with a much higher speciation rate in the subfamily Stenodermatinae (mean = 0.250 ± 0.032) than among background lineages (mean = 0.135 ± 0.015; figure 2*a*).

### (b) *Trait evolution*

The PC analysis of species means identified three PCs with eigenvalues of more than 1 (table 1). Species with low scores on PC1 (representing 49% of variation among species) exhibit short skulls, palates and coronoid processes coupled with relatively tall skulls and mandibular condyles (figure 3). The skulls of species with low PC2 scores (representing 24% of variation among species) are relatively wide and support large molars. PC3 represented only 11 per cent of variation among species and was not used in further analyses.

We found that both the first and second PC were significant predictors of trophic level ($\chi^2_1 = 8.46$, $p = 0.0130$ and $\chi^2_1 = 3.06$, $p = 0.0494$, respectively; figure 3*a*), supporting the prediction that trophic level and skull morphology (PCs) should be strongly associated. Those regressions rejected BM in favour of BM with the scaling parameter $\lambda$ as the best-fit model of evolution of residuals ($\lambda = 0.60 \pm 0.06$, $\chi^2_1 = 5.68$, $p = 0.0098$). Models of bite force on the PCs did not reject the BM model of evolution for error structure ($\chi^2_1 = 0.12$, $p = 0.7248$). The first PC significantly predicted bite force ($\chi^2_1 = 12.02$, $p = 0.0003$; figure 3*b*), but the second PC did not ($\chi^2_1 = 0.43$, $p = 0.4981$). All analyses that included bite force accounted for the strong positive relationship between bite force and head size ($\chi^2_1 = 38.43$, $p = 2.912\text{E-}10$; figure 3*b*).

As expected when rapidly filling new niches, trophic level in Stenodermatine bats evolved 3.515 ± 0.224 times faster than in other phyllostomids ($\chi^2_1 = 9.93$, $p = 0.0009$; figure 2*b*). Conversely, the skull morphology of Stenodermatine bats evolved 2.353 ± 0.266 times more slowly than in other phyllostomids ($\chi^2_1 = 7.33$, $p = 0.0038$; figure 2*c*). The Stenodermatinae occupied a significantly different trophic level relative to other phyllostomids ($\chi^2_1 = 9.22$, $p = 0.0013$), with a lower trophic level, more frugivorous diet (mean coefficient effect of being a stenodermatine on ln trophic level = −0.340 ± 0.012). We used a BM model of evolution for the error structure of residuals as it was not rejected in these models ($\chi^2_1 = 2.09$, $p = 0.0976$).

### (c) *Relationship between diversification and trait evolution*

Speciation rate increased nonlinearly with the proportion of fruit in the diet (i.e. as trophic level decreased, figure 4*a*). Trophic level decreased forward in time across the tree (directional tendency of trophic level in time, time increases backwards = 0.022 ± 0.002) in the best-fit model of evolution for this trait. This model was significantly better than the null model of constant tree-wide birth–death rates ($\chi^2_2 = 16.29$, $p = 0.0012$). The second-best model

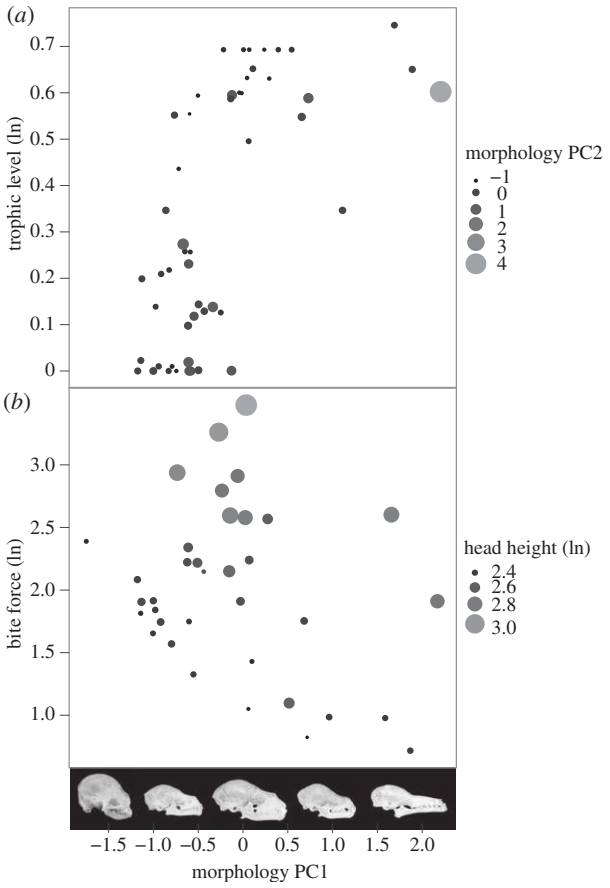


Figure 3. PC1 as a predictor of ln trophic level (*a*, mean coefficient = 0.193 ± 0.015) and ln bite force (*b*, mean coefficient = −0.327 ± 0.007). Symbols represent species means, and the size of the symbols indicate the magnitude of the significant, independent contributions of PC2 to ln trophic level (*a*, mean coefficient = −0.081 ± 0.015) and ln head height to ln bite force (*b*, mean coefficient = 2.826 ± 0.034). The relationships were modelled using GLS fitted with ML and phylogeny-based correlation structures of the errors. The relationship between skull morphology and PC1 scores are illustrated from left to right by: *Centurio senex*, *Carollia perspicillata*, *Phyllostomus elongatus*, *Micronycteris hirsuta*, *Choeronycteris mexicana*.

was linear and well supported ($\Delta AIC_{HMLL} = 0.408$, see the electronic supplementary material, table S6), and described speciation rate decreasing with increasing trophic level (figure 4*a*).

Speciation rate was lowest near PC1 values of 0.4, and increased nonlinearly as PC1 decreased or increased (figure 4*b*, see the electronic supplementary material, table S7). PC1 decreased forward in time across the tree (directional tendency of PC1 in time, time increases backwards = 0.138 ± 0.037). This model was significantly better than the null model of constant tree-wide birth–death rates ($\chi^2_2 = 15.84$, $p = 0.0014$); however, it converged only for 41 per cent of the trees examined (see the electronic supplementary material, table S7), and few species were available to estimate parameters at high PC1 values (figure 4*b*). For this reason, we also report the second best, poorly supported ($\Delta AIC_{ML} = 6.04$, see the electronic supplementary material, table S7), linear model in which speciation rate decreased with increasing PC1 values (figure 4*b*). Both models shared high speciation rates at low PC1 values.

## 4. DISCUSSION

### (a) *Diversification rate increased significantly in tandem with frugivory*

If relatively hard canopy fruits were an ecological opportunity that offered a new adaptive zone, then a clade that could access this new adaptive zone would shift its diet significantly and could diversify at a high rate. As predicted, we found a significant increase in speciation rate at the base of the highly frugivorous sternodermatine clade (figure 1). We were also able to demonstrate that the stenodermatine diet contains significantly more fruit than that of other phyllostomids. These results suggest strong clade-based links between ecological opportunity and diversification [10].

### (b) *Morphology predicts feeding performance and diet*

If morphology of the skull in stenodermatine bats conferred an advantage in the new adaptive zone, morphology had to predict feeding performance. We found that PC1 scores were significant predictors of bite force after adjusting for head size (figure 3*b*). The low PC1 scores typical of stenodermatines were a significant predictor of relatively high bite forces, so even absolutely small species have strong bites. This is probably because a shorter skull (and a shorter out lever, the distance from the teeth to the jaw joint), and perhaps differences in the jaw adductor muscles, confer increased mechanical advantage to stenodermatine skulls [23].

What is the advantage of a skull phenotype that confers increased bite force for these frugivores? Stenodermatines are unique in that even small species exploit relatively hard fruits, especially figs [22,60,61]. Other frugivorous phyllostomid lineages consume soft fruits and remain species poor (e.g. Carolliinae and Rhinophyllinae, see figure 1). Only stenodermatines have the ability to consume the entire range of fruit diversity available (i.e. both soft and hard fruits) in the new adaptive zone, and therefore benefit from the ecological opportunity of dedicated frugivory.

Both PC1 and PC2 were significant predictors of trophic level, with PC1 explaining more variation in trophic level than PC2 (figure 3*a*). This confirmed the predicted association between skull morphology and diet. We suspect that the mechanistic basis of the link between low PC1 scores (short skulls) and low trophic level values (more fruit) is mechanical advantage. There is no obvious mechanistic basis for the significant relationship between PC2 and trophic level, but the factor loadings on PC2 (table 1) suggest a role for a wider skull and larger molar teeth. Expanded crushing surfaces on molars are also associated with frugivory in both carnivorans and primates [62,63], suggesting a similar 'frugivore' morphotype has evolved multiple times in mammalian evolutionary history.

### (c) *Change in diet and skull shape underlie the increased species diversification rate*

The modelled relationships between diet (trophic level), skull shape (PC1) and tree-wide speciation rates are consistent with the hypothesis that the shift to a frugivorous diet which included hard fruits, and the evolution of a stouter skull promoted diversification. Differences in the rates of evolution in skull morphology and diet before and after the largest shift in diversification rates suggest

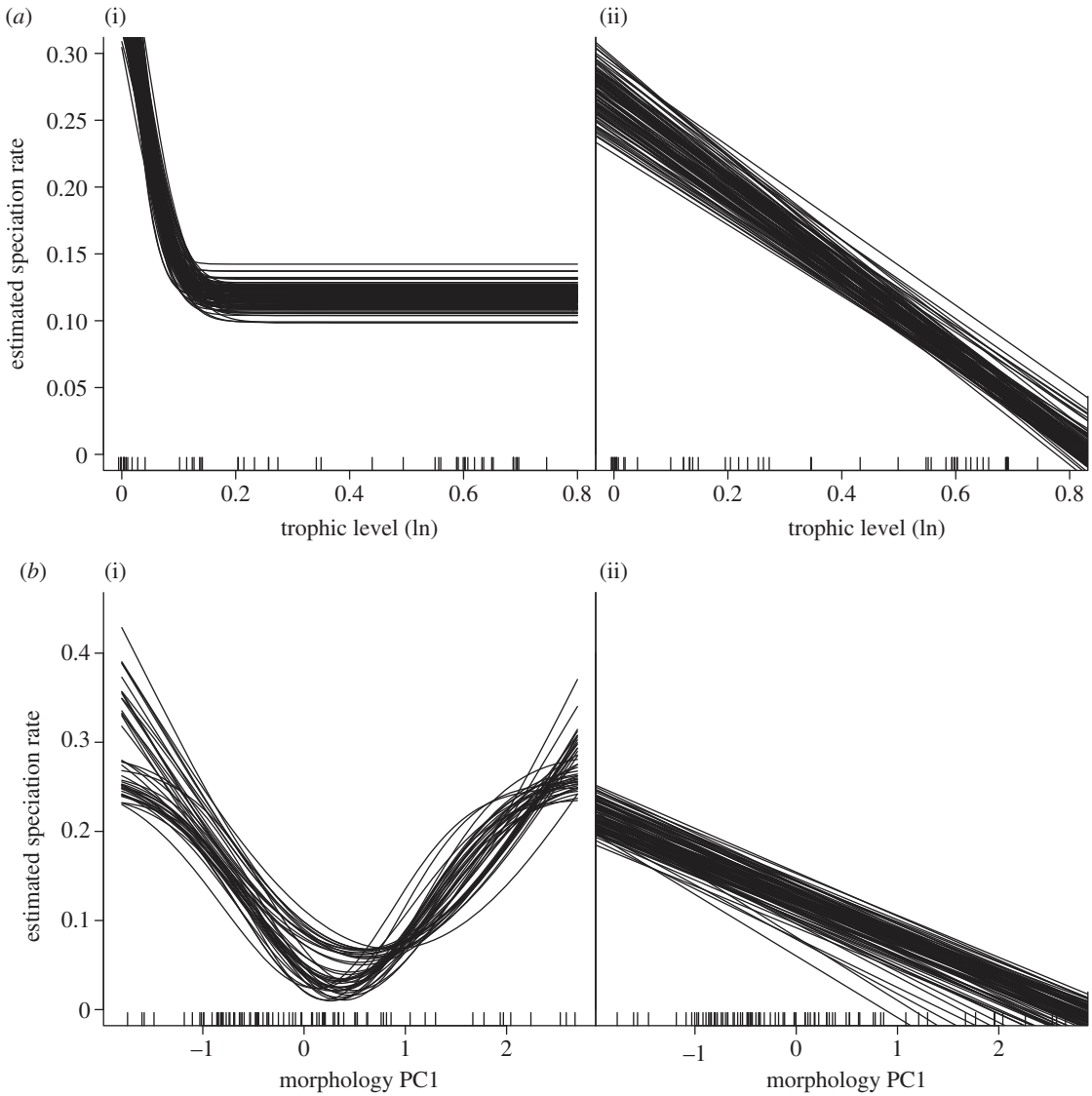


Figure 4. Best-fit models of speciation as a function of trait evolution for 100 phylogenies. (*a*) Ln trophic level: (i) nonlinear model (mean highest speciation rate: 0.409 ± 0.028 attained at −0.030 ± 0.011 on the ln trophic level axis; mean lowest speciation rate: 0.118 ± 0.008); and (ii) linear model (mean intercept speciation rate: 0.263 ± 0.016, mean coefficient speciation rate on ln trophic level: −0.311 ± 0.023). (*b*) PC1: (i) nonlinear model (mean lowest speciation rate: 0.038 ± 0.020 attained at 0.442 ± 0.154 on the PC1 axis; mean highest speciation rate: 0.424 ± 0.223); and (ii) linear model (mean intercept speciation rate: 0.122 ± 0.016, mean coefficient speciation rate on ln trophic level: −0.048 ± 0.005). Observed trait values are shown as ticks on the *x*-axes.

that morphological innovation and its effect on feeding performance may have played a leading role. We found that the rate of morphological evolution was slower after this shift than before it, as predicted if morphology reached a threshold of functionality and then remained in a plateau as it evolved minor variations on an effective theme [64]. In complement, we found that the rate of evolution in trophic level was higher after the shift in diversification rates than before it. This would be expected if the rate of trophic evolution accelerated as the new adaptive zone was quickly filled [7].

Morphological innovation as a catalyst for diversification has received a great deal of attention. Examples include the evolution of the hypocone (a cusp on the molar teeth of mammals) and nectar spurs on columbines [12,64,65]. Likewise, we found support for the hypothesis that the evolution of a skull phenotype which improved biting performance when eating hard fruits (a new adaptive zone) was associated with increasing diversification rates in phyllostomid bats. The novel skull phenotype of stenodermatines may also fulfil the definition of a 'key innovation'. We have linked the phenotype to heightened performance (enhanced bite force), and the role of performance in exploiting the new adaptive zone (hard fruits) has already been established [22–24]. Our results support the hypothesis that changes in skull morphology enabled the expansion of dietary niches in stenodermatines. Like all phyllostomid bats, stenodermatines have retained the ability to capture and consume insects and occasionally do so [50]. Unlike other phyllostomids, stenodermatines have the added capacity to consume both soft and hard fruits. Thus the range of dietary niches available to stenodermatine bats is effectively broader than that of other phyllostomids. We have not demonstrated that increased bite force is associated with increased fitness in bats, but this is within the realm of possibility, as exposure to tougher foods has been identified as the agent of selection for

higher bite forces in a population of lizards [66]. There is only a single instance of convergent evolution of a morphological innovation linked to dedicated frugivory in bats (species in the family Pteropodidae), and that system has not been investigated in sufficient detail to draw close parallels. Hence, we currently lack the replication necessary to propose the 'frugivore' skull as a key innovation. Nevertheless, our analyses support a central role for a novel skull phenotype in access to the ecological opportunity afforded by hard fruits, and thereby species diversification within phyllostomids.

Work with live animals was approved by Animal Care and Use Committee at the University of Massachusetts at Amherst (bite force) and the Leibniz Institute for Zoo and Wildlife Research (collection of faecal samples).

We thank Angelique S.P. Corthals, Amy L. Russell and Nancy B. Simmons for comments on this manuscript, Rich FitzJohn for support with DIVERSITREE, Alex Pyron for support with BEAST, Doug Futuyma and Jeff Levinton for insightful discussion, Gavin Thomas for an insightful review, and Marko Tschapka for permission to use photographs of *Lonchorhina aurita* and *Musonycteris harrisoni*. Kendra Cornejo and Alison Onstine photographed phyllostomid skulls at the AMNH Mammalogy collections, and N.B. Simmons provided access to these. The University of Oslo Bioportal provided computational support for early versions of the manuscript. This work was supported by grants to E.R.D. (NSF IOB 0447616 and NSF DBI 0743460), L.M.D. (NSF DEB 0206336) and S.S. (David J. Klingener Endowment Scholarship, Smithsonian Tropical Research Institute Predoctoral Fellowship).

## REFERENCES

1 Darwin, C. R. 1859 *On the origin of species by means of natural selection, or the preservation of favoured races in the struggle for life*, 1st edn. London, UK: John Murray.
2 Simpson, G. G. 1944 *Tempo and mode in evolution*. New York, NY: Columbia University Press.
3 Losos, J. B. 2010 Adaptive radiation, ecological opportunity, and evolutionary determinism. *Am. Nat.* **175**, 623–639. (doi:10.1086/652433)
4 Rabosky, D. L. & Glor, R. E. 2010 Equilibrium speciation dynamics in a model adaptive radiation of island lizards. *Proc. Natl Acad. Sci. USA* **107**, 22 178–22 183. (doi:10.1073/pnas.1007606107)
5 Bininda-Emonds, O. R. P. *et al.* 2007 The delayed rise of present-day mammals. *Nature* **446**, 507–512. (doi:10.1038/nature05634)
6 Rabosky, D. L. & Lovette, I. J. 2008 Density-dependent diversification in North American wood warblers. *Proc. R. Soc. B* **275**, 2363–2371. (doi:10.1098/rspb.2008.0630)
7 Schluter, D. 2000 *The ecology of adaptive radiation*. Oxford, UK: Oxford University Press.
8 Moore, B. R. & Donoghue, M. J. 2009 A Bayesian approach for evaluating the impact of historical events on rates of diversification. *Proc. Natl Acad. Sci. USA* **106**, 4307–4312. (doi:10.1073/pnas.0807230106)
9 Coyne, J. A. & Orr, H. A. 2004 *Speciation*. Sunderland, MA: Sinauer Associates.
10 Heard, S. B. & Hauser, D. L. 1995 Key evolutionary innovations and their ecological mechanisms. *Historical Biol. Int. J. Paleobiol.* **10**, 151–173.
11 Hunter, J. P. 1998 Key innovations and the ecology of macroevolution. *Trends Ecol. Evol.* **13**, 31–36. (doi:10.1016/S0169-5347(97)01273-1)
12 von Hagen, K. B. & Kadereit, J. W. 2003 The diversification of *Halenia* (Gentianaceae): ecological opportunity versus key innovation. *Evolution* **57**, 2507–2518. (doi:10.1111/j.0014-3820.2003.tb01495.x)
13 Alfaro, M., Brock, C., Banbury, B. & Wainwright, P. 2009 Does evolutionary innovation in pharyngeal jaws lead to rapid lineage diversification in labrid fishes? *BMC Evol. Biol.* **9**, 255. (doi:10.1186/1471-2148-9-255)
14 Yoder, J. B. *et al.* 2010 Ecological opportunity and the origin of adaptive radiations. *J. Evol. Biol.* **23**, 1581–1596. (doi:10.1111/j.1420-9101.2010.02029.x)
15 Rundell, R. J. & Price, T. D. 2009 Adaptive radiation, nonadaptive radiation, ecological speciation and nonecological speciation. *Trends Ecol. Evol.* **24**, 394–399. (doi:10.1016/j.tree.2009.02.007)
16 Mayr, E. 1963 *Animal species and evolution*. Cambridge, MA: Harvard University Press.
17 Van Bocxlaer, I., Loader, S. P., Roelants, K., Biju, S. D., Menegon, M. & Bossuyt, F. 2010 Gradual adaptation toward a range-expansion phenotype initiated the global radiation of toads. *Science* **327**, 679–682. (doi:10.1126/science.1181707)
18 Calsbeek, R. & Smith, T. B. 2008 Experimentally replicated disruptive selection on performance traits in a Caribbean lizard. *Evolution* **62**, 478–484. (doi:10.1111/j.1558-5646.2007.00282.x)
19 Rex, K., Michener, R., Kunz, T. H. & Voigt, C. C. 2011 Vertical stratification of neotropical leaf-nosed bats (Chiroptera: Phyllostomidae) revealed by stable carbon isotopes. *J. Trop. Ecol.* **27**, 211–222. (doi:10.1017/S0266467411000022)
20 Giannini, N. P. & Kalko, E. K. 2004 Trophic structure in a large assemblage of phyllostomid bats in Panama. *Oikos* **105**, 209–220. (doi:10.1111/j.0030-1299.2004.12690.x)
21 Freeman, P. W. 2000 Macroevolution in Microchiroptera: recoupling morphology and ecology with phylogeny. *Evol. Ecol. Res.* **2**, 317–335.
22 Aguirre, L. F., Herrel, A., Van Damme, R. & Matthysen, E. 2003 The implications of food hardness for diet in bats. *Funct. Ecol.* **17**, 201–212. (doi:10.1046/j.1365-2435.2003.00721.x)
23 Santana, S. E., Dumont, E. R. & Davis, J. L. 2010 Mechanics of bite force production and its relationship to diet in bats. *Funct. Ecol.* **24**, 776–784. (doi:10.1111/j.1365-2435.2010.01703.x)
24 Dumont, E. R., Herrel, A., Medellín, R. A., Vargas-Contreras, J. A. & Santana, S. E. 2009 Built to bite: cranial design and function in the wrinkle-faced bat. *J. Zool.* **279**, 329–337. (doi:10.1111/j.1469-7998.2009.00618.x)
25 Jones, K. E., Bininda-Emonds, O. R. P., Gittleman, J. L. & Yoder, A. 2005 Bats, clocks, and rocks: diversification patterns in Chiroptera. *Evolution* **59**, 2243–2255. (doi:10.1554/04-635.1)
26 Freckleton, R. P., Phillimore, A. B. & Pagel, M. 2008 Relating traits to diversification: a simple test. *Am. Nat.* **172**, 102–115. (doi:10.1086/588076)
27 Paradis, E. 2005 Statistical analysis of diversification with species traits. *Evolution* **59**, 1–12. (doi:10.1554/04-231)
28 Santana, S. E. & Dumont, E. R. 2009 Connecting behaviour and performance: the evolution of biting behaviour and bite performance in bats. *J. Evol. Biol.* **22**, 2131–2145. (doi:10.1111/j.1420-9101.2009.01827.x)
29 Gavrilets, S. & Losos, J. B. 2009 Adaptive radiation: contrasting theory with data. *Science* **323**, 732–737. (doi:10.1126/science.1157966)
30 Baker, R. J., Porter, C. A., Hoofer, S. R. & Van Den Bussche, R. A. 2003 A new higher-level classification of New World leaf-nosed bats based on nuclear and mitochondrial DNA sequences. *Occasional Pap. Mus. Texas Tech. Univ.* **230**, 1–32.

31 Teeling, E. C., Madsen, O., Murphy, W. J., Springer, M. S. & O'Brien, S. J. 2003 Nuclear gene sequences confirm an ancient link between New Zealand's short-tailed bat and South American noctilionoid bats. *Mol. Phylogenet. Evol.* **28**, 308–319. (doi:10.1016/S1055-7903(03)00117-9)

32 Bininda-Emonds, O. R. P. 2005 TransAlign: using amino acids to facilitate the multiple alignment of protein-coding DNA sequences. *BMC Bioinformatics* **6**, 156. (doi:10.1186/1471-2105-6-156)

33 Katoh, K. & Toh, H. 2008 Improved accuracy of multiple ncRNA alignment by incorporating structural information into a MAFFT-based framework. *BMC Bioinformatics* **9**, 212. (doi:10.1186/1471-2105-9-212)

34 McGuire, J. A., Witt, C. C., Altshuler, D. L. & Remsen Jr, J. V. 2007 Phylogenetic systematics and biogeography of hummingbirds: Bayesian and maximum likelihood analyses of partitioned data and selection of an appropriate partitioning strategy. *Syst. Biol.* **56**, 837–856. (doi:10.1080/10635150701656360)

35 Ronquist, F. & Huelsenbeck, J. P. 2003 MrBayes 3: Bayesian phylogenetic inference under mixed models. *Bioinformatics* **19**, 1572–1574. (doi:10.1093/bioinformatics/btg180)

36 Stamatakis, A. 2006 RAxML-VI-HPC: maximum likelihood-based phylogenetic analyses with thousands of taxa and mixed models. *Bioinformatics* **22**, 2688–2690. (doi:10.1093/bioinformatics/btl446)

37 Posada, D. & Buckley, T. R. 2004 Model selection and model averaging in phylogenetics: advantages of Akaike information criterion and Bayesian approaches over likelihood ratio tests. *Syst. Biol.* **53**, 793–808. (doi:10.1080/10635150490522304)

38 Nylander, J. A. A. 2004 *MrAIC.pl.* Uppsala: Evolutionary Biology Centre Uppsala University. Program distributed by the author.

39 Drummond, A. & Rambaut, A. 2007 Beast: Bayesian evolutionary analysis by sampling trees. *BMC Evol. Biol.* **7**, 214. (doi:10.1186/1471-2148-7-214)

40 Suchard, M. A. & Rambaut, A. 2009 Many-core algorithms for statistical phylogenetics. *Bioinformatics* **25**, 1370–1376. (doi:10.1093/bioinformatics/btp244)

41 Teeling, E. C., Springer, M. S., Madsen, O., Bates, P., O'Brien, S. J. & Murphy, W. J. 2005 A molecular phylogeny for bats illuminates biogeography and the fossil record. *Science* **307**, 580–584. (doi:10.1126/science.1105113)

42 Miller-Butterworth, C. M., Murphy, W. J., O'Brien, S. J., Jacobs, D. S., Springer, M. S. & Teeling, E. C. 2007 A family matter: conclusive resolution of the taxonomic position of the long-fingered bats *Miniopterus*. *Mol. Biol. Evol.* **24**, 1553–1561. (doi:10.1093/molbev/msm076)

43 Drummond, A. J., Ho, S. Y. W., Phillips, M. J. & Rambaut, A. 2006 Relaxed phylogenetics and dating with confidence. *PLoS Biol.* **4**, e88. (doi:10.1371/journal.pbio.0040088)

44 Rambaut, A. & Drummond, A. J. 2007 *Tracer*, v. 1.5. See http://tree.bio.ed.ac.uk/software/tracer/.

45 Burnham, K. P. & Anderson, D. R. 2002 *Model selection and multimodel inference*. New York, NY: Springer.

46 R Development Core Team 2011 *R: a language and environment for statistical computing*, v. 2.13.2. Vienna, Austria: R Foundation for Statistical Computing.

47 Rabosky, D. L. 2006 Laser: a maximum likelihood toolkit for detecting temporal shifts in diversification rates from molecular phylogenies. *Evol. Bioinformatics Online* **2**, 273–276.

48 FitzJohn, R. G., Maddison, W. P. & Otto, S. P. 2009 Estimating trait-dependent speciation and extinction rates from incompletely resolved phylogenies. *Syst. Biol.* **58**, 595–611. (doi:10.1093/sysbio/syp067)

49 Plummer, M., Best, N., Cowles, K. & Vines, K. 2006 Coda: convergence diagnosis and output analysis for MCMC. *R news* **6**, 7–11.

50 Rex, K., Czaczkes, B. I., Michener, R., Kunz, T. H. & Voigt, C. C. 2010 Specialization and omnivory in diverse mammalian assemblages. *Ecoscience* **17**, 37–46. (doi:10.2980/17-1-3294)

51 Jungers, W. L., Falsetti, A. B. & Wall, C. E. 1995 Shape, relative size, and size-adjustments in morphometrics. *Am. J. Phys. Anthropol.* **38**, 137–161. (doi:10.1002/ajpa.1330380608)

52 Dumont, E. R. & Herrel, A. 2003 The effects of gape angle and bite point on bite force in bats. *J. Exp. Biol.* **206**, 2117–2123. (doi:10.1242/jeb.00375)

53 Anderson, R. A., McBrayer, L. D. & Herrel, A. 2008 Bite force in vertebrates: opportunities and caveats for use of a nonpareil whole-animal performance measure. *Biol. J. Linn. Soc.* **93**, 709–720. (doi:10.1111/j.1095-8312.2007.00905.x)

54 Grafen, A. 1989 The phylogenetic regression. *Phil. Trans. R. Soc. Lond. B* **326**, 119–157. (doi:10.1098/rstb.1989.0106)

55 Paradis, E., Claude, J. & Strimmer, K. 2004 APE: analyses of phylogenetics and evolution in R language. *Bioinformatics* **20**, 289–290. (doi:10.1093/bioinformatics/btg412)

56 Pinheiro, J., Bates, D., DebRoy, S., Sarkar, D. & the R Core team 2009 *NLME: linear and nonlinear mixed effects models*, v. 3.1-96. See http://cran.r-project.org/web/packages/nlme.

57 Pagel, M. 1997 Inferring evolutionary processes from phylogenies. *Zool. Scr.* **26**, 331–348. (doi:10.1111/j.1463-6409.1997.tb00423.x)

58 O'Meara, B. C., Ané, C., Sanderson, M. J., Wainwright, P. C. & Hansen, T. 2006 Testing for different rates of continuous trait evolution using likelihood. *Evolution* **60**, 922–933. (doi:10.1554/05-130.1)

59 FitzJohn, R. G. 2010 Quantitative traits and diversification. *Syst. Biol.* **59**, 619–633. (doi:10.1093/sysbio/syq053)

60 Kalko, E. K. V. & Handley, C. O. 2001 Neotropical bats in the canopy: diversity, community structure, and implications for conservation. *Plant Ecol.* **153**, 319–333. (doi:10.1023/A:1017590007861)

61 Dumont, E. R. 1999 The effect of food hardness on feeding behaviour in frugivorous bats (Phyllostomidae): an experimental study. *J. Zool.* **248**, 219–229. (doi:10.1111/j.1469-7998.1999.tb01198.x)

62 Popowics, T. E. 2003 Postcanine dental form in the Mustelidae and Viverridae (Carnivora: Mammalia). *J. Morphol.* **256**, 322–341. (doi:10.1002/jmor.10091)

63 Boyer, D. 2008 Relief index of second mandibular molars is a correlate of diet among prosimian primates and other euarchontan mammals. *J. Hum. Evol.* **55**, 1118–1137. (doi:10.1016/j.jhevol.2008.08.002)

64 Hunter, J. P. & Jernvall, J. 1995 The hypocone as a key innovation in mammalian evolution. *Proc. Natl Acad. Sci. USA* **92**, 10 718–10 722. (doi:10.1073/pnas.92.23.10718)

65 Ree, R. H. & Yoder, A. 2005 Detecting the historical signature of key innovations using stochastic models of character evolution and cladogenesis. *Evolution* **59**, 257–265. (doi:10.1554/04-369)

66 Herrel, A., De Smet, A., Aguirre, L. F. & Aerts, P. 2008 Morphological and mechanical determinants of bite force in bats: do muscles matter? *J. Exp. Biol.* **211**, 86–91. (doi:10.1242/jeb.012211)

**Electronic supplementary material (ESM) for:**

Morphological innovation, diversification and the invasion of a new adaptive zone

Elizabeth R Dumont et al.

**Files in this Data Supplement:**

**Table ESM1.** Prior calibrations (in MYA) used to parameterize MCMCMC analyses of tree topology, rates of molecular evolution, and divergence times. Low boundaries were set to constrain the minimal age of the stratum where the fossil was found

| Source | Fossil age | Location in Figure ESM1 | Low boundary | 95% CI | Mean (stdv) |
|---|---|---|---|---|---|
| MRCA *Mystacina*/*Artibeus* [1] | — | Prior on age of root | — | 41-51 | 46 (2.5) |
| Stem mormoopid [2] | Late Oligocene (Arikareean) | 1 (includes stem) | 30.8 | 30.8-36.9 | 31(3) |
| *Desmodus archaeodaptes* [3] | Early Pleistocene (Early Irvingtonian) | 2 | 0.3 | 0.3-11.4 | 1.58 (5) |
| *Notonycteris* [4] | Middle Miocene (Laventan) | 3 (includes stem) | 11.8 | 11.8-18.1 | 12.2 (3) |
| *Tonatia* or *Lophostoma sp*. [4] | Middle Miocene (Laventan) | 4 (includes stem) | 11.8 | 11.8-18.1 | 12.2 (3) |
| *Palynephyllum antimaster* [4] | Middle Miocene (Laventan) | 5 (includes stem) | 11.8 | 11.8-18.1 | 12.2 (3) |
| *Phyllonycteris major* [5] | Quaternary | 6 | 0.001 | 0.001-10.7 | 0.905 (5) |
| *Brachyphylla nana* [6] | Quaternary | 7 [7] | 0.001 | 0.001-10.7 | 0.905 (5) |
| *Cubanycteris* [8] | Quaternary | 8 (includes stem) [9] | 0.001 | 0.001-10.7 | 0.905 (5) |
| *Phyllops vetus* [6] | Quaternary | 9 [10] | 0.001 | 0.001-10.7 | 0.905 (5) |

**Table ESM2.** Terminals in phylogeny with >1 species assigned in diversification rate analyses.

| Species in phylogeny | Spp. richness | Additional species |
|---|---|---|
| *Anoura caudifer* | 2 | *A. aequatoris* [11] |
| *Anoura geoffroyi* | 2 | *A. cultrata* |
| *Anoura latidens* | 2 | *A. luismanueli* |
| *Artibeus lituratus* | 2 | *A. anthonyi* [12] |
| *Carollia brevicauda* | 2 | *C. subrufa* |
| *Carollia perspicillata* | 2 | *C. colombiana* |
| *Choeroniscus minor* | 2 | *C. periosus* |
| *Desmodus rotundus* | 3 | *D. archeodaptes* [13], *draculae* [3], *stocki* [14] |
| *Glyphonycteris sylvestris* | 2 | *G. behni* |
| *Hylonycteris underwoodi* | 3 | *Lichonycteris obscura, Scleronycteris ega* |
| *Lampronycteris brachyotis* | 2 | *Neonycteris pusilla* |
| *Leptonycteris curasoae* | 2 | *L. nivalis* |
| *Lonchophylla chocoana* | 2 | *L. orcesi* [15, 16] |
| *Lonchophylla mordax* | 5 | *L. concava, fornicata, bokermanni, hesperia* [17] |
| *Lonchophylla robusta* | 2 | *L. orienticollina* [18] |
| *Lonchophylla thomasi* | 3 | *L. cadenai, pattoni* [19] |
| *Lonchorhina aurita* | 2 | *L. fernandezi* |
| *Lonchorhina orinocensis* | 2 | *L. marinkellei* |
| *Macrotus waterhousii* | 3 | *M. jamaicensis, M. compressus* [20] |
| *Mimon crenulatum* | 3 | *M. cozumelae, koepckeae* |
| *Phyllonycteris aphylla* | 2 | *P. major* |
| *Phyllops falcatus* | 3 | *P. silvai, vetus* [9] |
| *Phyllostomus elongatus* | 2 | *P. latifolius* |
| *Platalina genovensium* | 2 | *Xeronycteris vierai* [21] |
| *Platyrrhinus dorsalis* | 2 | *P. chocoensis* [22] |
| *Platyrrhinus helleri* | 2 | *P. umbratus* |
| *Sturnira erythromos* | 2 | *S. mistratensis* [23] |
| *Sturnira ludovici* | 2 | *S. sorianoi* [24] |

**Table ESM3.** Species means of tropic level (TL), sample sizes ($n_{TL}$), locality data and sampling period (LS, La Selva Biological Station, Costa Rica, 10°25'52“ N, 84°00'12“ W; TBS, Tiputini Biodiversity Station, Ecuador, 0°38.31' S, 76°8.92' W; BOM, Bombuscaro River, Podocarpus National Park Ecuador, 4°1’ S, 79°1’ W).

| | TL | $n_{TL}$ | Locality (sampling period) |
|---|---|---|---|
| *Anoura caudifer* | 1.93 ± .183 | 6 | BOM (Feb-Apr, Sept-Nov) |
| *Artibeus jamaicensis* | 1.6 | 4 | LS, TBS (Feb-Apr) |
| *Artibeus lituratus* | 1.18 | 11 | LS (Feb-Apr, Oct-Dec), TBS (Feb-Apr, Sep-Nov) |
| *Artibeus obscurus* | 1.32 | 18 | TBS (Feb-Apr, Sep-Nov) |
| *Artibeus phaeotis* | 1.2 | 5 | BOM (Feb-Apr, Sep-Nov), LS (Feb-Apr, Oct-Dec) |
| *Artibeus planirostris* | 1.36 | 40 | TBS (Feb-Apr, Sep-Nov) |
| *Artibeus watsoni* | 1.28 | 21 | LS (Feb-Apr, Oct-Dec) |
| *Carollia brevicauda* | 1.13 | 140 | BOM (Feb-Apr, Sep-Nov), TBS (Feb-Apr, Sep-Nov) |
| *Carollia castanea* | 1.16 | 85 | BOM (Feb-Apr, Sep-Nov), LS (Feb-Apr, Oct-Dec), TBS (Feb-Apr, Sep-Nov) |
| *Carollia perspicillata* | 1.17 | 43 | LS (Feb-Apr, Oct-Dec), TBS (Feb-Apr) |
| *Carollia sowelli* | 1.2 | 44 | LS (Feb-Apr, Oct-Dec) |
| *Chiroderma trinitatum* | 1.36 | 3 | TBS (Feb-Apr, Sep-Nov) |
| *Chiroderma villosum* | 1.86 | 7 | LS (Oct-Dec), TBS (Feb-Apr) |
| *Chrotopterus auritus* | 2.0 | 3 | BOM (Sep-Nov), TBS (Feb-Apr) |
| *Desmodus rotundus* | 1.84 | 2 | BOM (Feb-Apr, Sep-Nov) |
| *Ectophylla alba* | 1.8 | 5 | LS (Feb-Apr, Oct-Dec) |
| *Enchisthenes hartii* | 1.0 | 1 | |
| *Glossophaga commissarisi* | 1.78 | 4 | Ls (Oct-Dec), TBS (Feb-Apr) |
| *Glossophaga soricina* | 1.84 | 11 | TBS (Feb-Apr, Sep-Nov) |
| Lampro*nycteris brachyotis* | 2.0 | 1 | |
| *Lonchophylla thomasi* | 1.5 | 2 | TBS (Feb-Apr) |
| *Lophostoma carrikeri* | 2.0 | 3 | BOM (Feb-Apr, Sep-Nov) |
| *Lophostoma silvicolum* | 1.85 | 34 | LS (Oct-Dec), TBS (Feb-Apr, Sep-Nov) |
| *Mesophylla macconnelli* | 1.94 | 7 | Ls (Oct-Dec), TBS (Feb-Apr, Sep-Nov) |
| *Metavampyressa_nymphaea* | 1.0 | 1 | |

| | | | |
|---|---|---|---|
| *Micronycteris hirsuta* | 1.89 | 8 | LS (Feb-Apr, Oct-Dec) |
| *Micronycteris megalotis* | 2.0 | 5 | BOM (Sep-Nov), LS (Oct-Dec) |
| Micronycteris_microtis | 2.0 | 1 | |
| *Micronycteris minuta* | 1.93 | 7 | LS (Feb-Apr), TBS (Feb-Apr) |
| *Mimon crenulatum* | 1.86 | 20 | LS (Feb-Apr), TBS (Feb-Apr, Sep-Nov) |
| *Phylloderma stenops* | 1.97 | 2 | TBS (Feb-Apr) |
| *Phyllostomus discolor* | 1.84 | 45 | LS (Feb-Apr, Oct-Dec) |
| *Phyllostomus elongatus* | 1.89 | 29 | TBS (Feb-Apr, Oct-Dec) |
| *Phyllostomus hastatus* | 1.67 | 22 | LS (Oct-Dec) |
| *Platyrrhinus brachycephalus* | 1.5 | 2 | TBS (Feb-Apr) |
| *Platyrrhinus helleri* | 1.01 | 7 | TBS (Feb-Apr, Sep-Nov) |
| *Platyrrhinus infuscus* | 1.00 | 2 | BOM (Feb-Apr, Sep-Nov) |
| *Rhinophylla fischerae* | 1.38 | 10 | TBS (Feb-Apr, Sep-Nov) |
| *Rhinophylla pumilio* | 1.02 | 31 | TBS (Feb-Apr, Sep-Nov) |
| *Sturnira erythromos* | 1.001 | 4 | BOM (Feb-Apr, Sep-Nov) |
| *Sturnira lilium* | 1.001 | 9 | BOM (Feb-Apr), TBS (Feb-Apr, Sep-Nov) |
| *Sturnira ludovici* | 1.001 | 15 | BOM (Feb-Apr, Sep-Nov) |
| *Sturnira luisi* | 1.05 | 8 | TBS (Feb-Apr) |
| *Sturnira magna* | 1.22 | 18 | TBS (Feb-Apr, Sep-Nov) |
| *Tonatia bidens* | 1.89 | 17 | TBS (Feb-Apr) |
| *Tonatia saurophila* | 2.0 | 6 | LS (Feb-Apr, Oct-Dec) |
| *Trachops cirrhosus* | 2.18 | 18 | LS (Oct-Dec), TBS (Feb-Apr, Sep-Nov) |
| *Uroderma bilobatum* | 1.26 | 2 | BOM (Feb-Apr), TBS (Feb-Apr) |
| *Vampyressa bidens* | 1.0 | 2 | TBS (Feb-Apr) |
| *Vampyressa thyone* | 1.02 | 5 | BOM (Feb-Apr, Sep-Nov), TBS (Feb-Apr) |

**Table ESM4**. Values and sample sizes for morphological PC1 and ($N_{MORPH}$) mean maximum bite force ($N_{BF}$), and mean head height used in comparative analyses. Morphological data were collected from specimens housed in the American Museum of Natural History, the Carnegie Museum of Natural History, and the National Museum of Natural History.

| Species | Morphology principal component 1 | $N_{MORPH}$ | Mean maximum bite force | Mean head height (mm) | $N_{BF}$ |
|---|---|---|---|---|---|
| *Ametrida centurio* | -1.58434 | 6 | - | - | - |
| *Anoura caudifer* | 1.95047 | 6 | - | - | - |
| *Anoura geoffroyi* | 1.67890 | 10 | 2.66 | 11.05 | 1 |
| *Ardops nichollsi* | -.90590 | 2 | - | - | - |
| *Ariteus flavescens* | -1.18557 | 6 | - | - | - |
| *Artibeus anderseni* | -1.01299 | 6 | - | - | - |
| *Artibeus cinereus* | -.87154 | 7 | - | - | - |
| *Artibeus concolor* | -.79463 | 4 | - | - | - |
| *Artibeus glaucus* | -.85455 | 6 | 6.79 | 11.64 | 6 |
| *Artibeus jamaicensis* | -.58428 | 16 | 18.92 | 17.76 | 196 |
| *Artibeus lituratus* | -.12760 | 6 | 26.15 | 19.83 | 24 |
| *Artibeus obscurus* | -.68786 | 6 | - | - | - |
| *Artibeus phaeotis* | -.83457 | 11 | 6.31 | 11.20 | 5 |
| *Artibeus planirostris* | -.51692 | 6 | - | - | |
| *Artibeus watsoni* | -.98372 | 6 | 6.73 | 12.16 | 17 |
| *Brachyphylla cavernarum* | .28629 | 10 | - | - | - |
| *Carollia brevicauda* | -.48259 | 15 | 9.24 | 12.29 | 28 |
| *Carollia castanea* | -.41743 | 11 | 3.77 | 11.08 | 11 |
| *Carollia perspicillata* | -.30643 | 10 | 8.56 | 12.69 | 63 |
| *Carollia sowelli* | -.36804 | 15 | - | - | |
| *Centurio senex* | -1.59039 | 10 | 10.91 | 10.42 | 26 |
| *Chiroderma trinitatum* | -.45840 | 6 | - | - | - |
| *Chiroderma villosum* | -.37524 | 10 | - | - | - |
| *Choeroniscus godmani* | 2.52422 | 4 | - | - | - |
| *Choeroniscus minor* | 2.65608 | 6 | - | - | - |
| *Choeronycteris mexicana* | 2.59028 | 6 | - | - | - |

| | | | | | |
|---|---|---|---|---|---|
| *Chrotopterus auritus* | .64154 | 7 | - | - | - |
| *Desmodus rotundus* | 2.25816 | 6 | 6.77 | 16.02 | 5 |
| *Diaemus youngi* | .33883 | 3 | - | - | - |
| *Diphylla ecaudata* | -.15464 | 5 | - | - | - |
| *Ectophylla alba* | -.46646 | 2 | 5.75 | 10.85 | 10 |
| *Enchisthenes hartii* | -1.02881 | 7 | 8.04 | 11.62 | 4 |
| *Erophylla sezekorni* | .63358 | 9 | 3.00 | 13.78 | 6 |
| *Glossophaga commissarisi* | .75099 | 5 | - | - | - |
| *Glossophaga longirostris* | 1.06673 | 6 | 2.68 | 11.30 | 4 |
| *Glossophaga soricina* | .82322 | 11 | 2.28 | 9.79 | 6 |
| *Hylonycteris underwoodi* | 2.03771 | 5 | - | - | - |
| *Leptonycteris nivalis* | 1.3048 | 4 | - | - | - |
| *Lichonycteris obscura* | 1.30554 | 4 | - | - | |
| *Lonchophylla robusta* | .79445 | 1 | 5.78 | 11.83 | 3 |
| *Lonchophylla thomasi* | 1.19374 | 5 | - | - | - |
| *Lophostoma brasiliense* | .19441 | 10 | 9.40 | 12.43 | 4 |
| *Lophostoma carrikeri* | .11938 | 7 | - | - | - |
| *Lophostoma silvicolum* | 0.07349 | 10 | 18.42 | 15.80 | 9 |
| *Macrotus californicus* | .54432 | 6 | - | - | - |
| *Macrotus waterhousii* | .51717 | 20 | - | - | - |
| *Mesophylla macconnelli* | -.63019 | 23 | - | - | - |
| *Micronycteris brachyotis* | .34451 | 10 | - | - | |
| *Micronycteris hirsuta* | .39852 | 20 | 13.06 | 13.52 | 3 |
| *Micronycteris megalotis* | .18107 | 20 | 2.86 | 10.00 | 4 |
| *Micronycteris microtis* | .49646 | 6 | - | - | - |
| *Micronycteris minuta* | .22085 | 5 | 4.18 | 10.47 | 2 |
| *Mimon crenulatum* | .09926 | 10 | 6.76 | 12.43 | 6 |
| *Monophyllus redmani* | 1.95380 | 6 | 2.05 | 11.19 | 2 |
| *Phylloderma stenops* | -.00533 | 3 | 13.43 | 17.60 | 4 |
| *Phyllonycteris poeyi* | .28588 | 4 | - | - | - |

| | | | | | |
|---|---|---|---|---|---|
| *Phyllostomus discolor* | -.02010 | 6 | 8.60 | 14.54 | 2 |
| *Phyllostomus elongatus* | .15787 | 10 | 13.21 | 16.48 | 10 |
| *Phyllostomus hastatus* | .17491 | 6 | 32.47 | 22.20 | 22 |
| *Platyrrhinus helleri* | -.65600 | 10 | 4.81 | 11.69 | 4 |
| *Platyrrhinus infuscus* | -.60983 | 6 | - | - | - |
| *Platyrrhinus lineatus* | -.80171 | 6 | - | - | - |
| *Platyrrhinus umbratus* | -.61490 | 1 | 6.23 | 11.75 | 3 |
| *Pygoderma bilabiatum* | -1.47121 | 9 | - | - | - |
| *Rhinophylla fischerae* | -.53605 | 6 | - | - | - |
| *Rhinophylla pumilio* | -.47739 | 8 | - | - | - |
| *Sphaeronycteris toxophyllum* | -1.75589 | 6 | - | - | - |
| *Stenoderma rufum* | -1.10039 | 2 | - | - | - |
| *Sturnira bidens* | -0.45288 | 2 | - | - | - |
| *Sturnira bogotensis* | -0.47602 | 10 | - | - | - |
| *Sturnira erythromos* | -.47119 | 6 | 10.40 | 13.00 | 5 |
| *Sturnira lilium* | -.36979 | 15 | 9.20 | 13.10 | 14 |
| *Sturnira ludovici* | -.01128 | 6 | 12.40 | 5 | - |
| *Sturnira luisi* | - | - | 10.00 | 13.42 | 3 |
| *Sturnira magna* | -.21341 | 6 | - | - | - |
| *Sturnira tildae* | -.26485 | 6 | - | - | - |
| *Tonatia saurophila* | -.09802 | 10 | 16.39 | 15.8 | 9 |
| *Trachops cirrhosus* | 1.75662 | 10 | 13.52 | 17.13 | 14 |
| *Uroderma bilobatum* | -.77458 | 10 | 5.73 | 11.86 | 15 |
| *Uroderma magnirostrus* | -.73500 | 6 | - | - | - |
| *Vampyressa bidens* | -.85996 | 6 | 5.23 | 10.90 | 2 |
| *Vampyressa nymphaea* | -.69329 | 4 | - | - | - |
| *Vampyressa thyone* | -.99520 | 5 | - | - | - |
| *Vampyrodes caraccioli* | -.81139 | 6 | - | - | - |
| *Vampyrum spectrum* | .86843 | 9 | - | - | - |

**Table ESM5.** Comparison of the harmonic mean of log-likelihoods (HMLL) sampled from MrBayes analyses of parameters (including a ML topology) fitted to the sequence data under different partition schemes. The ratio of parameters to partition varies, as optimal models for individual partitions ranged from a simple Jukes-Cantor model to the general-time-reversible model with gamma-distributed rates of change across sites.

| $N_{partitions}$ | Description | $N_{parameters}$ | HMLL | AIC*c* | BIC |
|---|---|---|---|---|---|
| 1 | Unpartitioned | 12 | -91006.77 | 3613627.01 | 182115.36 |
| 2 | Mt, nuclear | 21 | -90991.49 | 3618870.25 | 182161.16 |
| 3 | Mt rRNA, codon positions: 1+2, 3 | 32 | -89707.85 | 3527683.84 | 179687.21 |
| 4 | Mt rRNA, codon positions: 1, 2, 3 | 39 | -89595.02 | 3523925.55 | 179520.94 |
| 5 | Mt rRNA, codon positions: mt 1+2, 3; nuclear 1+2, 3 | 46 | -89391.94 | 3513250.82 | 179174.17 |
| 7 | Mt rRNA, codon positions: mt 1, 2, 3; nuclear 1, 2, 3 | 37 | -89301.91 | 3500102.99 | 178917.75 |

**Table ESM6.** Comparison of different models of the relationship of diversification as a function of trophic level fitted using ML. The best models fitted to one tree (bold and underlined), and those within 2 AIC units (bold) were then tested across a random sample of 100 trees, and summarized using the HMLL.

| Model | $N_{parameters}$ | ln Lik | AIC | $\chi^2_{null}$ | *P*-value | HMLL | $AIC_{HMLL}$ | $\chi^2_{HMLL}$ | *P*-value$_{HMLL}$ |
|---|---|---|---|---|---|---|---|---|---|
| Constant birth-death rates (null) | 3 | -100.128 | 206.26 | | | -100.809 | 207.618 | | |
| Speciation rate linear to trophic level | 4 | -95.269 | **198.54** | 9.7172 | 0.001825 | -96.064 | 200.128 | 9.4896 | 0.001126 |
| Speciation rate sigmoidal to trophic level | 6 | -96.422 | 204.84 | 7.4123 | 0.059854 | | | | |
| Speciation rate hump to trophic level | 6 | -94.121 | **200.24** | 12.0144 | 0.007334 | -94.686 | 201.372 | 12.2464 | 0.0030594 |
| Speciation rate linear to trophic level with direction parameter | 5 | -94.272 | **198.54** | 11.7110 | 0.002864 | -94.866 | 199.732 | 11.8866 | 0.0013117 |
| Speciation rate hump to trophic level with direction parameter | 7 | -92.196 | **<u>198.39</u>** | 15.8648 | 0.003206 | -92.662 | **<u>199.324</u>** | 16.2942 | 0.0011796 |
| Constant birth-death rates with split at Stenodermatinae | 5 | -94.734 | **199.37** | 10.7877 | 0.004545 | -95.418 | 200.837 | 10.7815 | 0.0059714 |
| Background speciation rate linear to trophic level, Stenodermatinae constant rates | 6 | -94.531 | 201.06 | 11.1936 | 0.010724 | | | | |
| Background constant rates, Stenodermatinae speciation rate linear to trophic level | 6 | -94.472 | 200.94 | 11.3128 | 0.010149 | | | | |
| Background and Stenodermatinae speciation rate linear to trophic level | 7 | -94.267 | 202.53 | 11.7219 | 0.019544 | | | | |

**Table ESM7.** Comparison of different models of the relationship of diversification as a function of morphological principal component 1 (PC1) fitted using ML. The best model fitted to one tree (bold and underlined), and those within 2 AIC units (bold) were then tested across a random sample of 100 trees, and summarized using the HMLL. Note: fitting hump models with direction parameter (bold and underlined under $AIC_{HMLL}$) converged for only 41 of 100 trees evaluated.

| Model | $N_{parameters}$ | ln Lik | AIC | $\chi^2_{null}$ | *P*-value | HMLL | $AIC_{HMLL}$ | $\chi^2_{HMLL}$ | *P*-value$_{HMLL}$ |
|---|---|---|---|---|---|---|---|---|---|
| Constant birth-death rates (null) | 3 | -234.38 | 474.76 | | | -238.69 | 483.38 | | |
| Speciation rate linear to PC1 | 4 | -230.66 | 469.32 | 7.4354 | 0.006395 | | | | |
| Speciation rate sigmoidal to PC1 | 6 | -226.33 | 464.67 | 16.0900 | 0.001087 | | | | |
| Speciation rate hump to PC1 | 6 | -226.54 | 465.08 | 15.6830 | 0.001317 | | | | |
| Speciation rate linear to PC1 with direction parameter | 5 | -224.15 | **458.31** | 20.4533 | 0.000036 | -235.78 | 481.56 | 5.8194 | 0.027246 |
| Speciation rate hump to PC1 with direction parameter | 7 | -222.28 | **458.57** | 24.7156 | 0.000073 | -230.76 | **475.52** | 15.8457 | 0.001435 |
| Constant birth-death rates with split at Stenodermatinae | 5 | -228.72 | 467.43 | 11.3247 | 0.003474 | | | | |
| Background speciation rate linear to PC1, Stenodermatinae constant rates | 6 | -228.66 | 469.31 | 11.4439 | 0.009552 | | | | |
| Background constant rates, Stenodermatinae speciation rate linear to PC1 | 6 | -228.51 | 469.02 | 11.7402 | 0.008328 | | | | |
| Background and Stenodermatinae speciation rate linear to PC1 | 7 | -228.45 | 470.90 | 11.8556 | 0.018458 | | | | |

**Figure ESM1**. Fossil calibration points on ML phylogram. See Table ESM1 for distribution of each constraint, confidence interval, and its phylogenetic position.

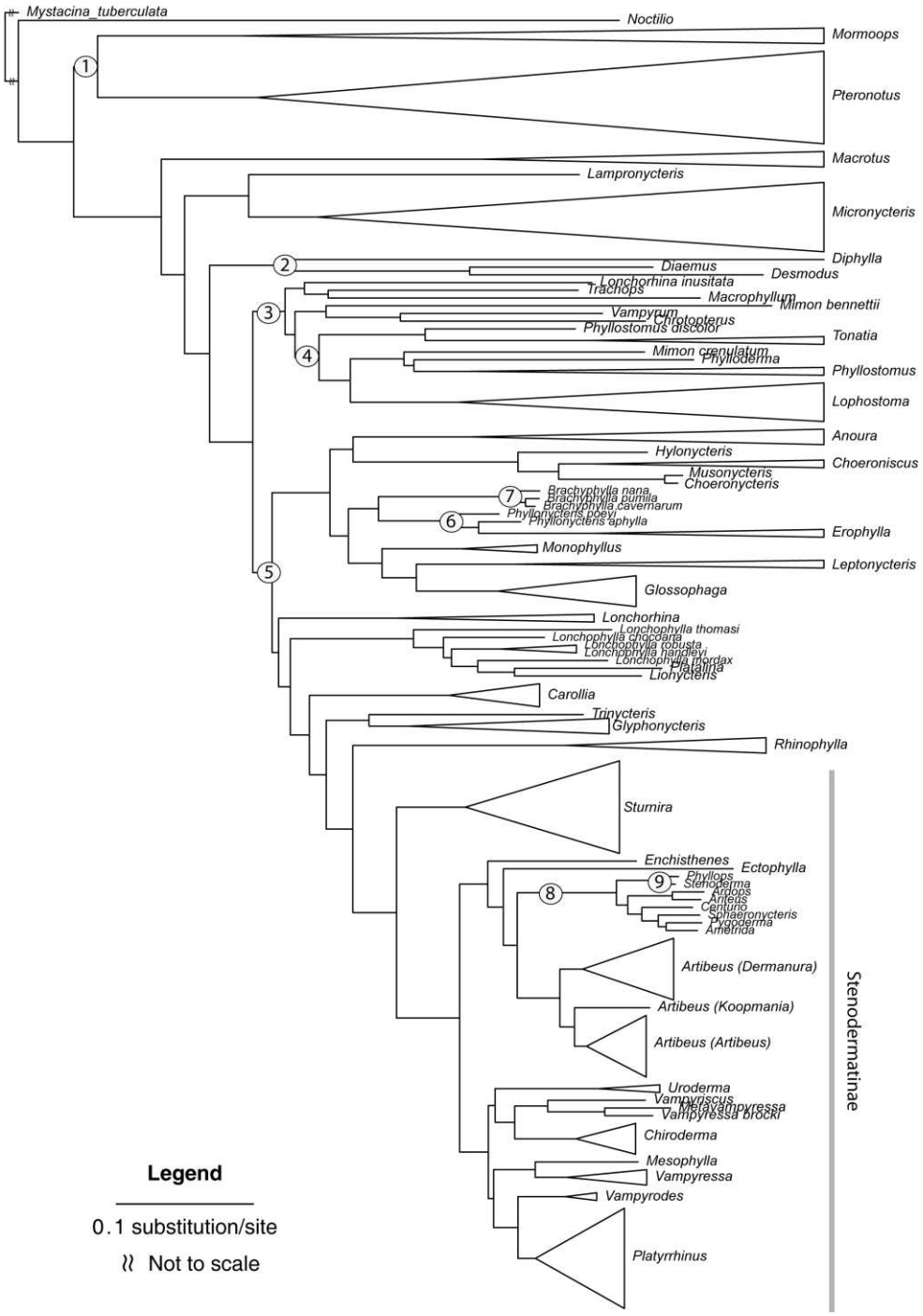

**Figure ESM2**. Summary of phylogenies and branch support based on posterior distribution of ultrametric trees. Branches without numeric support values had Bayesian posterior probabilities (BPP) of 1.0.

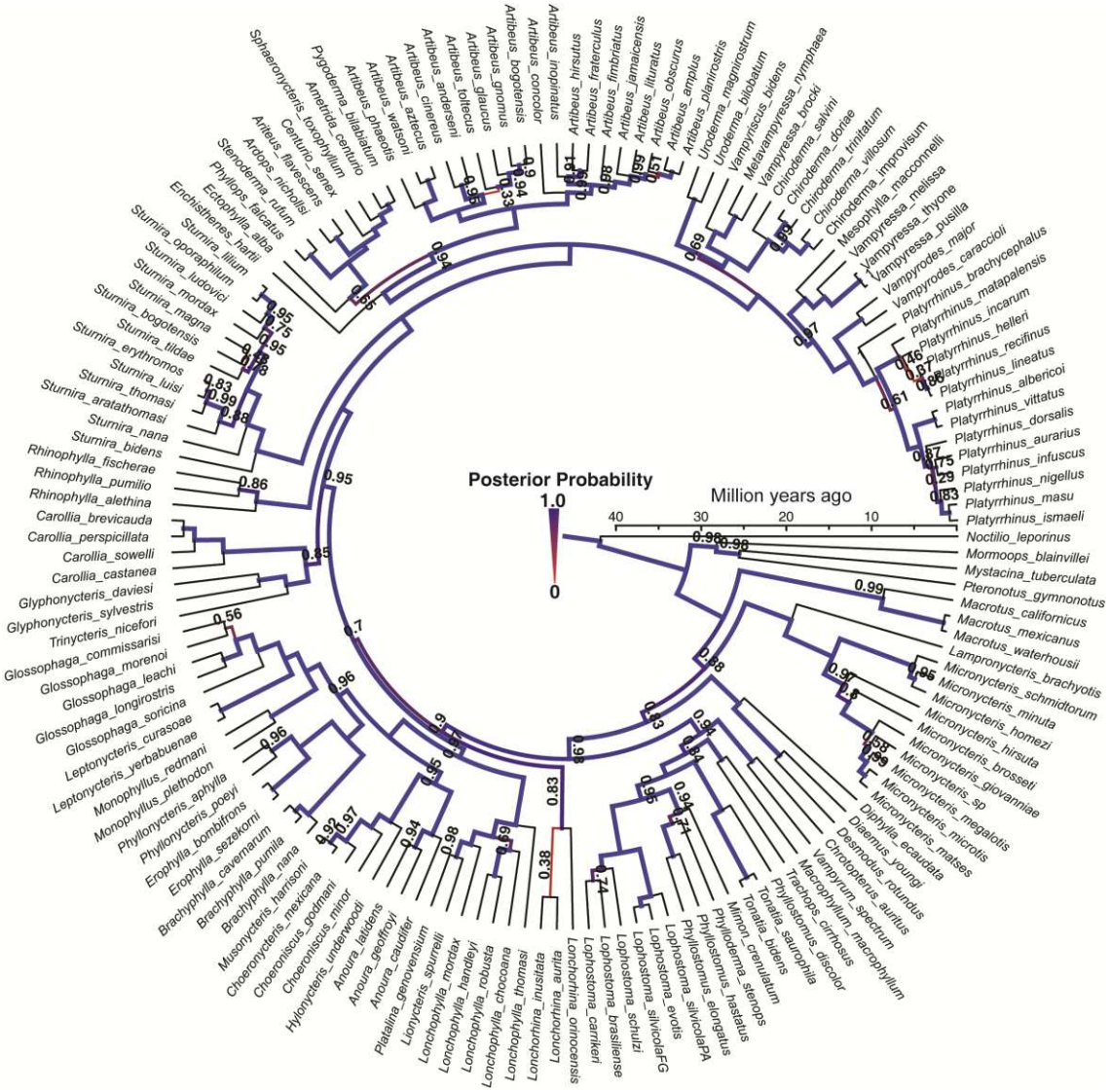

**Rferences**

1. Teeling, E. C., Springer, M. S., Madsen, O., Bates, P., O'Brien, S. J. & Murphy, W. J. 2005 A molecular phylogeny for bats illuminates biogeography and the fossil record. *Science* **307**, 580-584.
2. Czaplewski, N. J. & Morgan, G. S. 2003 Fossil bats of the Americas. Sam Noble Oklahoma Museum of Natural History; [cited 2010 19 October]; Available from: http://www.snomnh.ou.edu/collections%26research/vertebrate_paleontology/fossil_bats/index.shtml.
3. Morgan, G. S., Linares, O. J. & Ray, C. E. 1988 New species of fossil vampire bats (Mammalia: Chiroptera: Desmodontidae) from Florida and Venezuela. *Proc. Biol. Soc. Wash.* **101**, 912-928.
4. Czaplewski, N. J., Takai, M., Naeher, T. M., Shigehara, N. & Setoguchi, T. 2003 Additional bats from the middle Miocene La Venta fauna of Colombia. *Revista de la Academia Colombiana de Ciencias Exactas Fisicas y Naturales* **27**, 263-282.
5. Choate, J. R. & Birney, E. C. 1968 Sub-Recent Insectivora and Chiroptera from Puerto Rico, with the Description of a New Bat of the Genus *Stenoderma*. *Journal of Mammalogy* **49**, 400-412. (DOI 10.2307/1378198.)
6. Silva-Taboada, G. 1979 *Los murciélagos de Cuba*. La Habana: Editorial Academia.
7. Dávalos, L. M. 2010 Earth history and the evolution of Caribbean bats. In *Island bats: ecology, evolution, and conservation* (eds. T. H. Fleming & P. A. Racey), pp. 96-115. Chicago: University of Chicago Press.
8. Czaplewski, N. J., Krejca, J. & Miller, T. E. 2003 Late quaternary bats from Cebada Cave, Chiquibul Cave System, Belize. *Caribbean Journal of Science* **39**, 23-33.
9. Mancina, C. A. & Garcia-Rivera, L. 2005 New genus and species of fossil bat (Chiroptera: Phyllostomidae) from Cuba. *Caribb. J. Sci.* **41**, 22-27.
10. Dávalos, L. M. 2007 Short-faced bats (Phyllostomidae: Stenodermatina): a Caribbean radiation of strict frugivores. *J. Biogeogr.* **34**, 364-375. (doi:10.1111/j.1365-2699.2006.01610.x.)
11. Mantilla-Meluk, H. & Baker, R. J. 2006 Systematics of small *Anoura* (Chiroptera: Phyllostomidae) from Colombia, with description of a new species. *Occasional Papers, Museum of Texas Tech University* **261**, 1-18.
12. Woloszyn, B. W. & Taboada, G. S. 1977 Nueva especie fósil de *Artibeus* (Mammalia: Chiroptera) de Cuba, y tipificación preliminar de los depósitos fosilíferos Cubanos contentivos de mamíferos terrestres. *Poeyana* **161**.
13. Ray, C. E., Linares, O. J. & Morgan, G. S. 1988 Paleontology. In *Natural History of Vampire Bats* (eds. A. M. Greenhall & U. Schmidt), pp. 19-30. Boca Raton: CRC Press.
14. Jones, J. K., Jr. 1958 Pleistocene bats from San Josecito Cave, Nuevo León, México. *University of Kansas Publications, Museum of Natural History* **9**, 389-396.

15. Albuja V., L. & Gardner, A. L. 2005 A new species of *Lonchophylla* Thomas (Chiroptera: Phyllostomidae) from Ecuador. *Proc. Biol. Soc. Wash.* **118**, 442-449.
16. Dávalos, L. M. 2004 A new Chocoan species of *Lonchophylla*. *Am. Mus. Novit.* **3426**, 1-14.
17. Woodman, N. 2007 A new species of nectar-feeding bat, genus *Lonchophylla*, from western Colombia and western Ecuador (Mammalia Chiroptera: Phyllostomidae). *Proc. Biol. Soc. Wash.* **120**, 340-358.
18. Dávalos, L. M. & Corthals, A. 2008 A new species of *Lonchophylla* (Chiroptera: Phyllostomidae) from the eastern Andes of northwestern South America. *Am. Mus. Novit.* **3635**, 1-16.
19. Woodman, N. & Timm, R. M. 2006 Characters and phylogenetic relationships of nectar-feeding bats, with descriptions of new *Lonchophylla* from western South America (Mammalia: Chiroptera: Phyllostomidae: Lonchophyllini). *Proc. Biol. Soc. Wash.* **119**, 437-476.
20. Fleming, T. H., Murray, K. L. & Carstens, B. C. 2010 Phylogeography and genetic structure of three evolutionary lineages of West Indian phyllostomid bats. In *Evolution, ecology, and conservation of island bats* (eds. T. H. Fleming & P. A. Racey), pp. Chicago: University of Chicago Press.
21. Gregorin, R. & Ditchfield, D. A. 2005 New genus and species of nectar-feeding bat in the tribe Lonchophyllini (Phyllostomidae: Glossophaginae) from northeastern Brazil. *J. Mammal.* **86**, 403-414.
22. Velazco, P. M. 2005 Morphological Phylogeny of the Bat Genus *Platyrrhinus* Saussure, 1860 (Chiroptera: Phyllostomidae) with the Description of Four New Species. *Fieldiana Zool.*, 1-53. (doi:10.3158/0015-0754(2005)105[1:MPOTBG]2.0.CO;2.)
23. Iudica, C. A. A Systematic Revision of the Neotropical Fruit Bats of the Genus Sturnira: a Molecular and Morphological Approach [Doctoral]. Gainesville, FL: University of Florida; 2000.
24. Sánchez-Hernández, C., Romero-Almaraz, M. L. & Schnell, G. D. 2005 New species of *Sturnira* (Chiroptera: Phyllostomidae) from northern South America. *J. Mammal.* **86**, 866-872. (doi:10.1644/1545-1542(2005)86[866:NSOSCP]2.0.CO;2.)